International Journal of Science and Research (IJSR)
ISSN (Online): 2319-7064
Index Copernicus Value (2015): 78.96 | Impact Factor (2015): 6.391

# Influence of Number Shots of Laser on Structural Transformations and Optical Properties of ZnS Nanoparticles Thin Films

**A. Z. Mohammed[1], N. J. Mohammed[2], I. K. Khudhair[3]**

[1, 3]Physics Department, Faculty of Science, Zagazig Univ., Zagazig, Egypt

[2]Physics Department, Faculty of Science, Al-Mustansiriyah Univ, Iraq

**Abstract:** ***Effects of no. shots of laser and annealing temperature on the structural, morphological, and optical properties of Zinc sulfide nanoparticles (ZnS NPs) thin films prepared by pulsed laser deposition technique (PLD) were investigated. ZnS NPs films were deposited on glass substrates at room temperature (300K) by different no. shots of laser (1000, 2000, 3000), annealed at 623K under vacuum with $10^{-5}$ mbar. Crystallite size of ZnS NPs films was investigated by XRD and morphological properties by AFM. Transformation in the shape of nanoparticles to nanoflowers and nanorods appeared with increasing no. shots of laser at the same annealing temperature (623K) was observed from scanning electron microscopy (SEM) images. Experimental results show that the as-deposited ZnS NPs film exhibiting cubic structure and the crystallinity increased in the films annealed. It is also found that grain size of as grown samples at 300K, rises linearly from (9- 11nm) with no. shots above about (1000- 3000) and rapidly from (10-18 nm) after annealing at 623K. Additionally, the increase of no. shots from (1000-3000) leads to decrease the energy gap values and increase their values after heat treatment with stay their behavior decreasing as the no. shots of laser increases. Also photoluminescence (PL) measurements explained quenching its value after annealing temperature.***

**Keywords:** ZnS, Pulsed laser deposition, Nanoparticles, Nanoleaves, nanoflowers, nanorods, Photoluminescence (PL), Annealing temperature

## 1. Introduction

ZnS is a II-VI compound semiconductor. It is widely applied in the optoelectronic applications consisting of light emitting diodes with short wavelength. The structure and properties of ZnS films are varies with different deposited technique. Many growth techniques have been reported to prepare ZnS thin films, such as sputtering [1], Pulsed-laser deposition [2], metal organic chemical vapor deposition [3], electron beam evaporation [4], photochemical deposition [5], and chemical bath deposition [6]. Among these methods, electron beam evaporation is the most interesting since the advantages of electron beam evaporation are stability, reproducibility; high deposition rate and the compositions of the films are controllable. ZnS is one of the first semiconductors discovered [7], and is also an important semiconductor material with direct wide band gaps for cubic and hexagonal phases of 3.72 and 3.77 eV , respectively [8]. It has a high absorption coefficient in the visible range of the optical spectrum and reasonably good electrical properties [9]. In recent years, ZnS thin films have been grown by a variety of deposition techniques, such as chemical bath deposition [10], evaporation [11], and solvo thermal method [12]. Chemical bath deposition is promising because of its low cost arbitrary substrate shapes, simplicity, and capability of large area preparation, there are many reports of successful fabrication of ZnS – based hetero-junction solar cells by the chemical bath deposition method, such as with CIGS used for the n-type emitter layer [13]. The much pulsed laser deposition experiments were carried out in the 1960s. But it was first during the 1980s that it was popularized by the work of Inamet et al [14], who deposited high temperature super conducting films with a complex stochiome ZnS is potentially important material to be used as an antireflection coating for hetero-junction solar cells [15]. In this research we have achieved a novel method by changing the no. shots of laser to produce ZnS NPs, nanoflowers and nanorods at the same heat treatment temperature (623K) without inlet gas to the vacuum chamber.

## 2. Experimental

The ceramic ZnS target used is a pellet with dimensions ( 2 cm x 0.1 cm), density 3.66 g /$cm^3$ and purity 99.99%, supplied by the Kurt J. Lesker Company. It is produced by pressing squeeze at (13) ton, and sintering ZnS powder under vacuum at 1125K. It is a suitable target for PLD since it is dense and flat, enabling uniform energy transfer to its surface and the absence of voids keeps large particles being ejected from the surface. ZnS NPs films were prepared by pulsed laser deposition system of ZnS pellet fixed to a target holder that located at 2 cm and parallel to the substrate surface. The PLD was carried out by using a Q-switched Nd: YAG laser with wave length (1064 nm), no. shots of laser (1000, 2000, 3000), laser flounce (16.98 J/$cm^2$) and spot (d=3mm) at an angle 0f 45$^o$. The repetition rate of the laser beam was 5 Hz. The target and substrate rotated with 10 and 6 rpm respectively, by using DC motor to avoid drilling effect. The chamber of substrate and target holder evacuated to a pressure about $10^{-5}$ mbar. The preparing temperatures of samples were as grown temperature (300K) and annealing temperature (623K). In a typical case (16.98 J/$cm^2$, 1064 nm) the thickness created after deposition by 1500 pulses was found to be 50 nm.


Licensed Under Creative Commons Attribution CC BY

## 3. Results & Discussion

The target of ZnS was investigated by X-ray diffraction as shown in the Fig.1, and found that ZnS exhibits hexagonal phase. ZnS NPs thin films were prepared in a chamber evacuated to a base pressure of ($10^{-5}$ mbar). All three films prepared by different no. shots of laser (1000, 2000, and 3000) at room temperature (300K) were annealed at 623K. The crystal structure of the films was examined by X-ray diffraction (XRD) as shown in the Fig. 2.

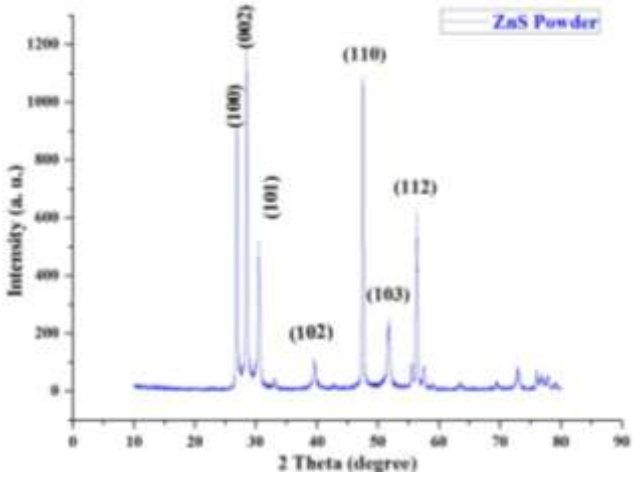


**Figure 1:** X-ray diffraction patterns for ZnSta target.

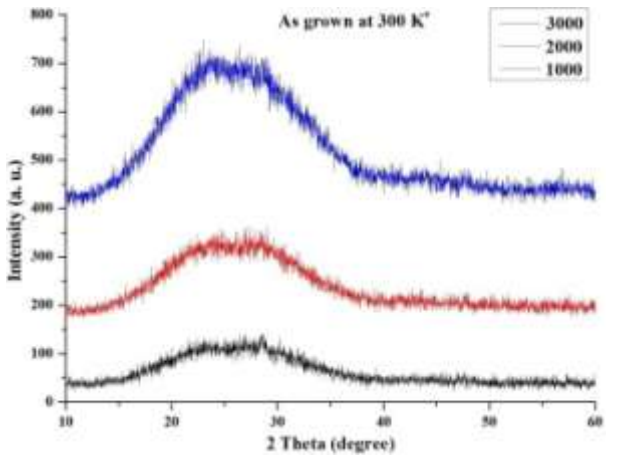


(a)

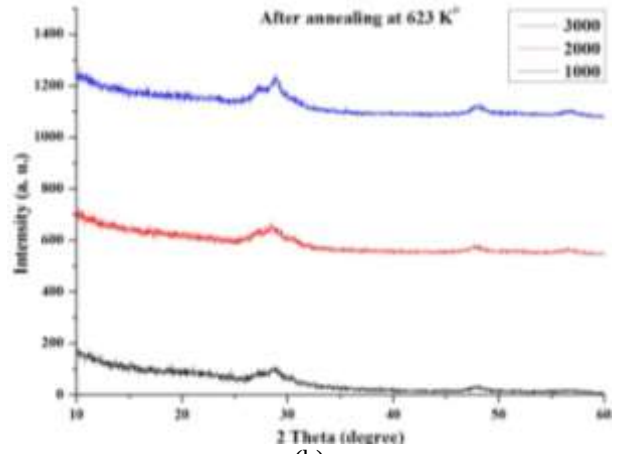


(b)

**Figure 2:** X-ray diffraction patterns for ZnS NPs films at a**)** as grown 300K, b**)** annealed at 623K

The average crystallite size ($D$) of ZnS NPs was estimated by the standard Scherrer formula [16]

$$D = \frac{k\lambda}{\beta cos\theta} \qquad (1)$$

Where $k$ is constant$(0.89 < k > 1)$, $\beta$ is the Full Width at Half Maximum (FWHM) of the diffraction peak, $\lambda$ is the wavelength of the X-ray and $\theta$ is diffraction angle. At different no. shots of laser (1000, 2000, 3000), it can be observed that the crystallite size of the samples increased after annealing from (9, 9.5, 11nm) at (300K) to (10, 11, 18 nm) at 623K.as shown in Fig.3.

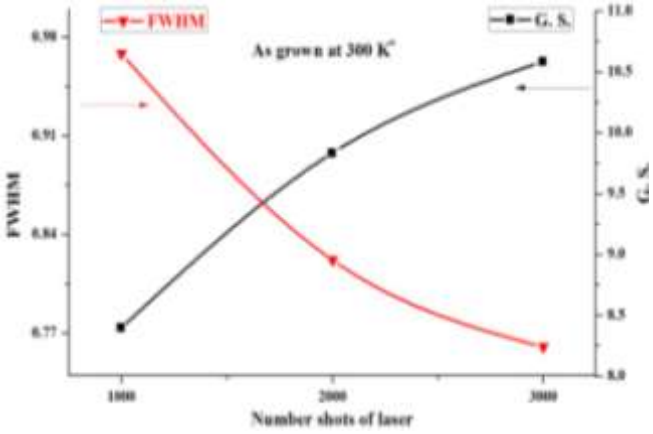


(a)

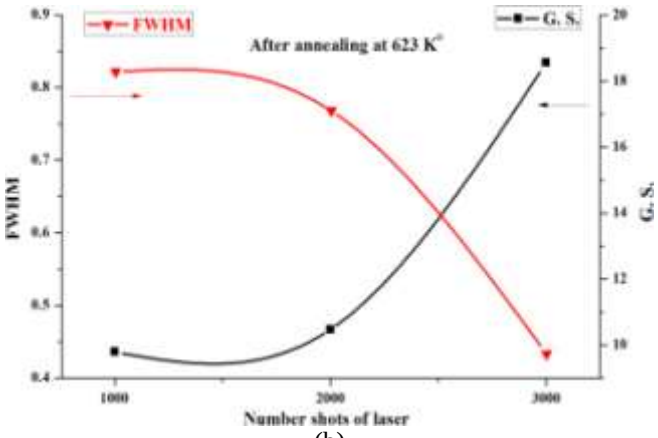


(b)

**Figure 3:** The crystallite size verse FWHM of ZnS NPs films for different no. shots (1000, 2000, 3000) at: **a)** as grown 300K, **b)** annealed at 623K.

Also, it can be noticed that the differences in the crystallite size at 300K and at annealed temperature (623K) increased with increasing no. of pulses as shown inFig 4.


Licensed Under Creative Commons Attribution CC BY

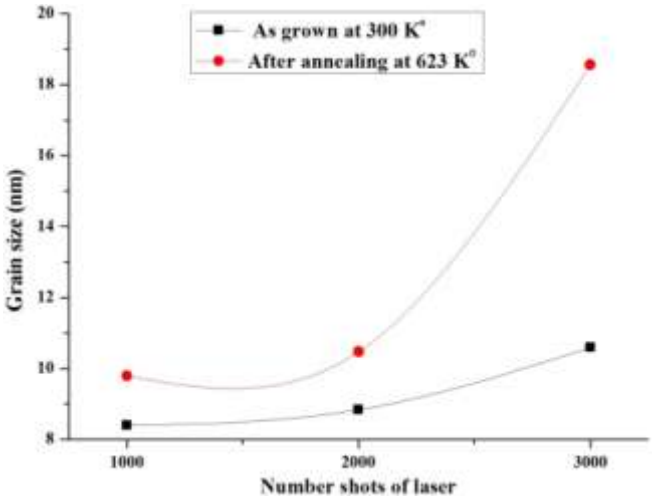


**Figure 4:** The differences in the crystallite size at 300K and at annealing temperature (623k)

Further investigations on the characteristics of nanosized structures of the deposited materials were achieved using atomic force microscopy. The AFM image of the ZnS NPs thin films deposited by different no. shots (1000, 2000, 3000) at 300K$^{o}$ are shown in Fig. 5.

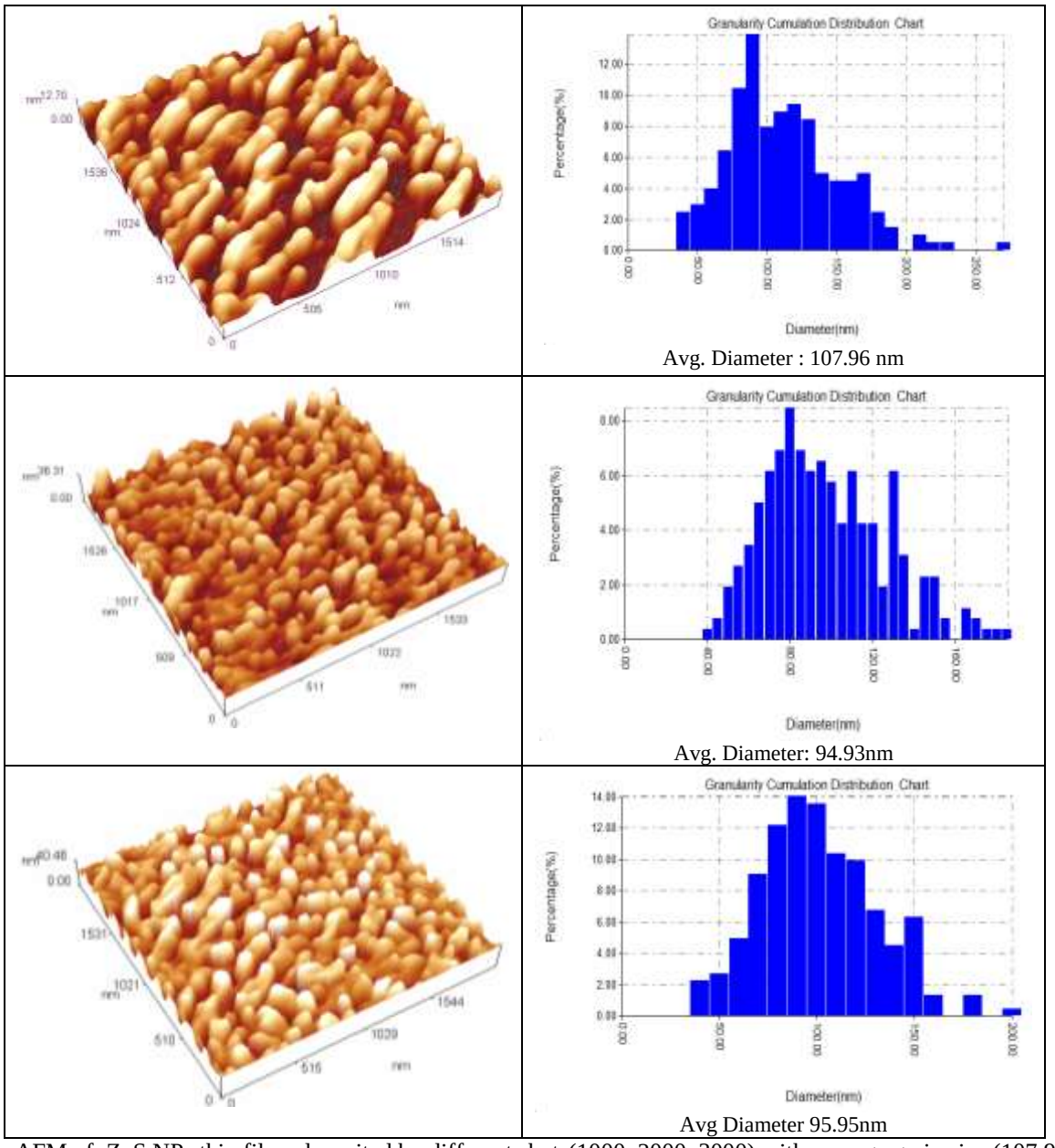


**Figure 5:** AFM of ZnS NPs thin films deposited by different shots(1000, 2000, 3000) with average grain size (107.96, 94.93 and 95.95nm) respectively before annealing(623k)

Also, The AFM image of the ZnS NPs thin films deposited by different no. shots (1000, 2000, and 3000) after annealed at 623K can be observed in the Fig. 6.


Licensed Under Creative Commons Attribution CC BY

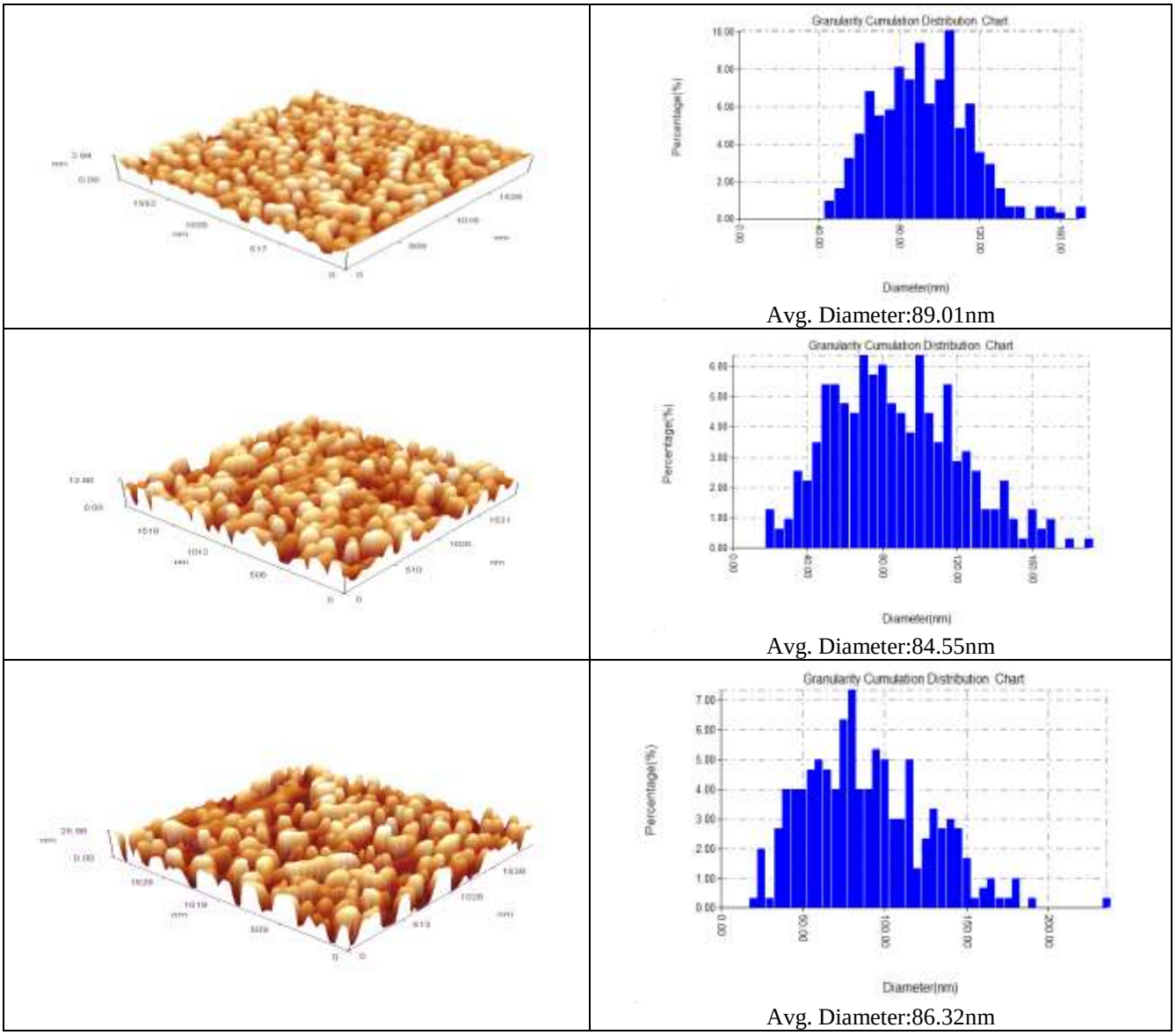


**Figure 6:** AFM of ZnS NPs thin films deposited by different shots (1000, 2000, 3000) with average grain size (89.01, 84.55 and 86.32 nm) respectively after annealing at 623K

The average size of ZnS NPs was about 99 nm at 300K and the average size decreased to 86 nm after annealing samples at 623K. The root mean square (rms) surface roughness at 300K for prepared films with different no. shots (1000, 2000, and 3000) are 3.61, 7.78 and 8.36 nm respectively. After annealed samples at 623K the (rms) surface roughness decreased for each sample and increased with increasing no. shots of laser for all samples. Table 1 shows the surface roughness of ZnS NPs thin film deposited on glass substrate. Increasing no. shots leads to an increased roughness of the surface and increasing the temperature could reduce it. The decrease in (rms) surface roughness may be due to less point defects which means a decrease of dislocations density (δ) in the films as shown in table 1.

**Table 1:** Shows that, surface roughness of ZnS NPs films prepared at temperature (300k) and (623k)

| Preparation temperature (K) | No. of laser shots | Root mean square surface roughness (nm) | Dislocations density(δ) $(nm)^{-2}$ |
|---|---|---|---|
| As grown at (300K) | 1000 | 3.61 | 0.0142 |
| | 2000 | 7.78 | 0.0103 |
| | 3000 | 8.36 | 0.0089 |
| After annealing at (623K) | 1000 | 0.674 | 0.0091 |
| | 2000 | 3.17 | 0.0059 |
| | 3000 | 7.47 | 0.0029 |

The SEM images are presented in Fig. 7 as a function of no. shots of laser and annealing temperature. Fig. 7(a) shows the SEM image of a synthesized sample at 300K for (1000 shots), the nanoparticles transformed to nanoflowers as a result of the accumulation of nano leaves generated by nanoparticles from the effect of heat treatment at 623K. We noticed that when the number of shots 2000, the nanoparticles take the form of nanorods with a diameter ranging from 50 to 150 nanometers with an increase in the number of shots to 3000 after annealing at 623K as


Licensed Under Creative Commons Attribution CC BY

illustrated by Fig. 7(b) and (c) respectively, are in the nanometer size supporting the diffraction result. Annealing of particles at various temperature results in an agglomeration of particles as shown in Fig. 4. At higher annealing temperatures, the nanoparticles are seen merging with each other and forming a neck between the two particles.

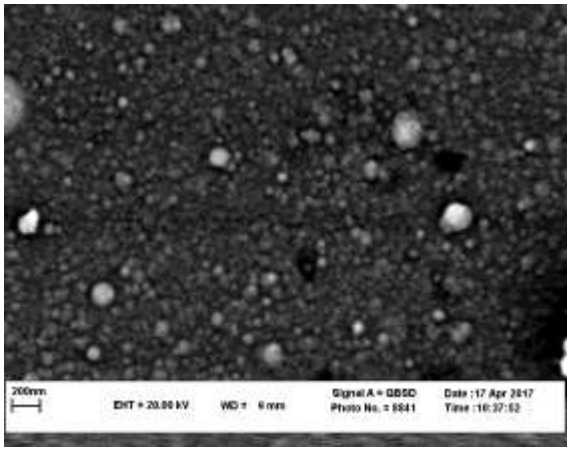

(a)Before annealing (300k) at (1000)p

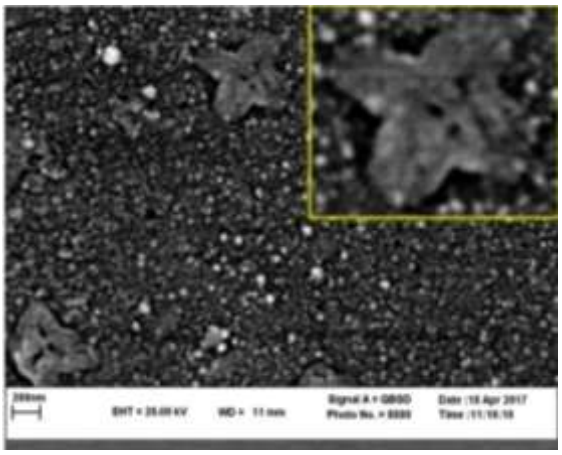

After annealing (623k) at (1000)p nanoflower

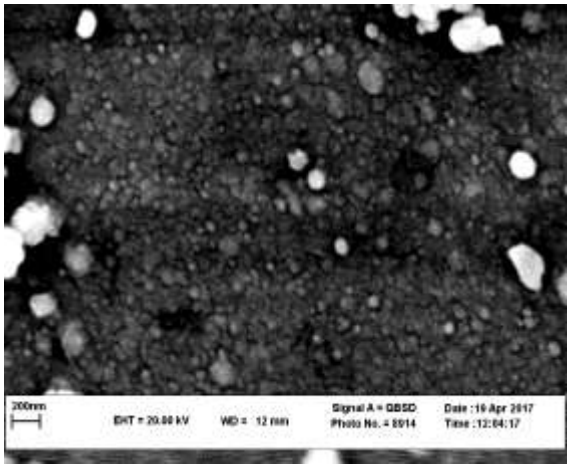

(a) Befor annealing (300k) at (2000)p

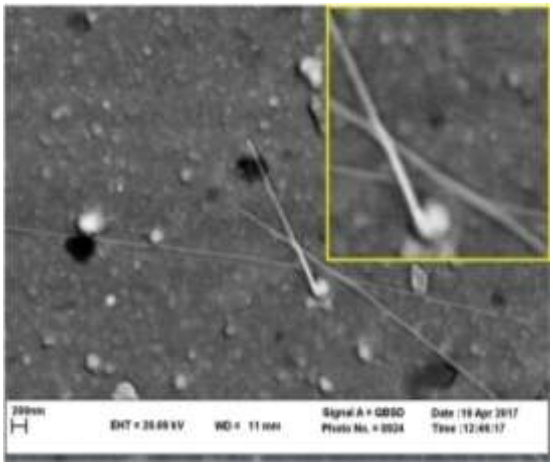

After annealing (623k) at (2000)p nanorod

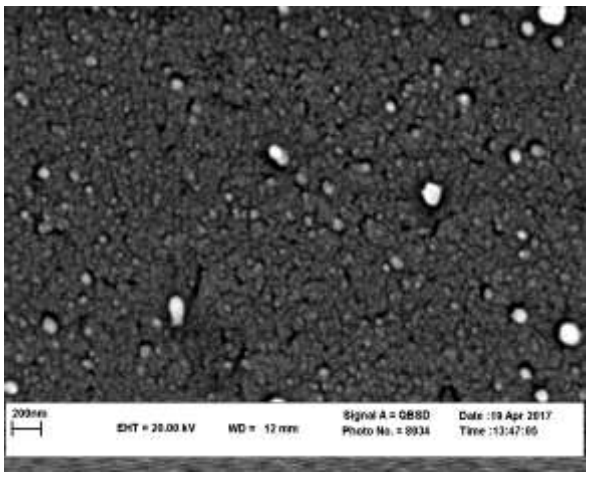

(c) before annealing (300k) at (3000)p

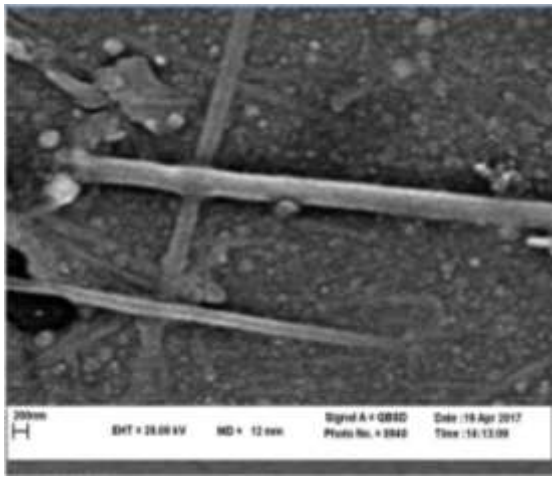

after annealing (623k) at (3000)p nanorod

**Figure 7:** SEM images of ZnS NPs thin films, the particles are shown for 1000 shots (a); and for 2000 shots (b); and for 3000 shots (c) at (300K) and annealing (623K)

Interference peaks in the Fig. 8. explained the uniform of the ZnS NPs films at 300K and the transmittance was found to increase with increasing no. shots of laser. after annealing at 623K.


Licensed Under Creative Commons Attribution CC BY

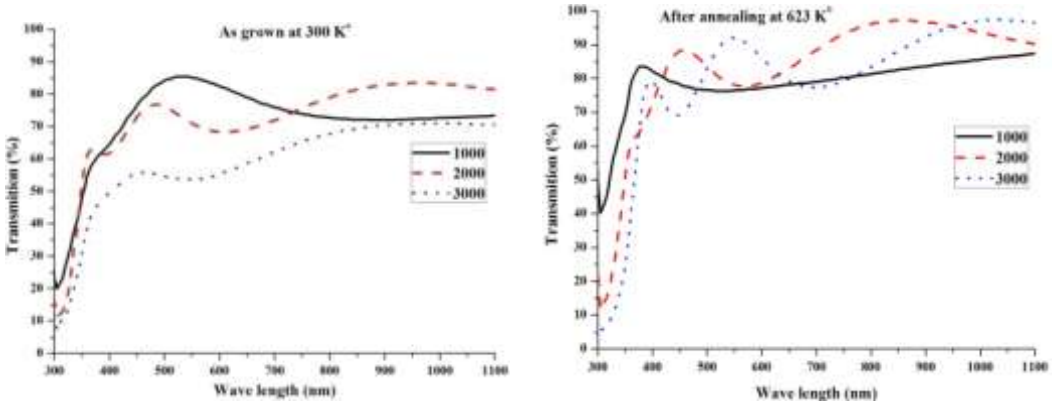


**Figure 8:** Optical transmission of the ZnS NPs films at 300K and annealed temperature (623K).

The direct energy band gap (Eg) was estimated from transmittance data as a function of wavelength using the relation [17]; $\alpha h\nu = (h\nu - E_g)^{\frac{1}{2}}$, where $h\nu$ is the photon energy (eV). The energy gap ($E_g$) of ZnS NPs films prepared at 300K and 623K calculated by extrapolating the linear part of $(\alpha h\nu)^2$ vs. $(h\nu)$ curves to $(\alpha h\nu)^2$=0 as shown in the Fig. 9.

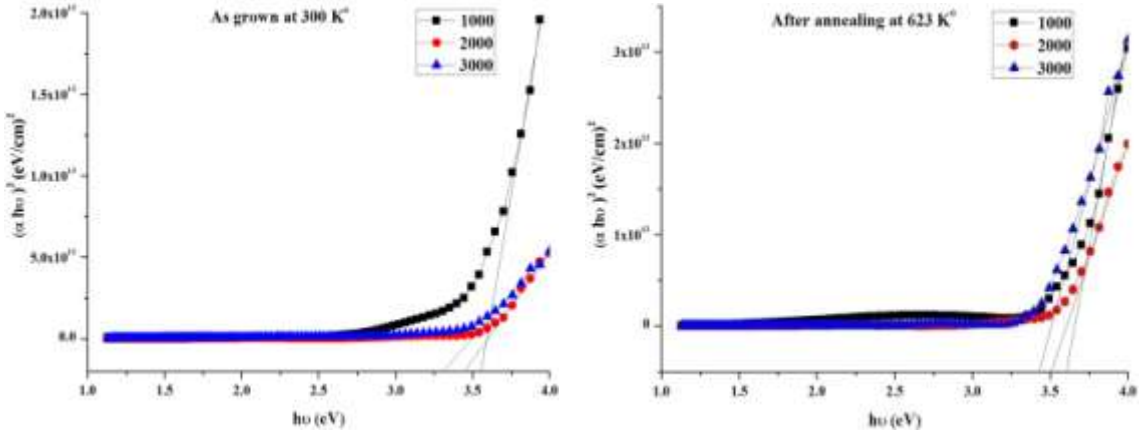


**Figure 9:** The energy gap ($E_g$) of ZnS NPs films prepared at 300K and 623K.

The band gap values estimated in this work for annealed ZnS NPs films at 623K (3.569, 3.488, 3.377 eV) are found to be higher than that prepared at 300K (3.557, 3.449, 3.319 eV), which may be linked with the structural changes causing quantum confinement effects in the ZnS NPs films as shown in Fig. 10.

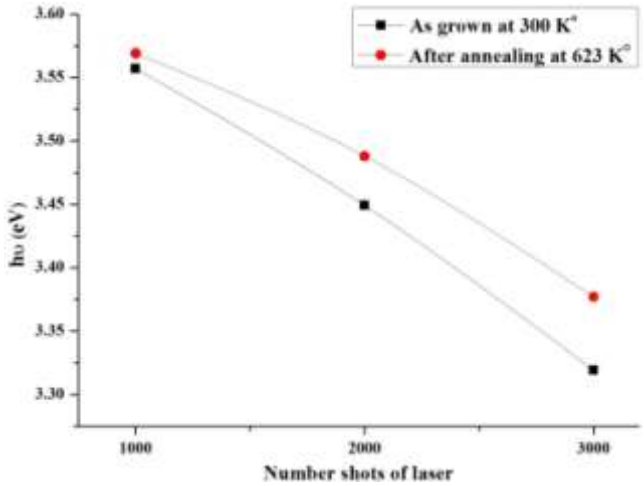


**Figure 10:** The $E_g$ of ZnS NPs films prepared at temperature 300K and 623K

Also the decrease in the values of Eg by increasing no. of laser shots (1000, 2000, 3000) is due to the increase in crystal size of ZnS NPs. Photoluminescence (PL) spectrum of ZnS NPs films, which was prepared with a number of laser shots (1000) and flounce (16.98 J/cm$^2$) at (300K) and annealed at 623K, was measured in the region from 350 to 700 nm with excitation wave length (350 nm). Fig.11 shows ZnS NPs films grown (300K), there are two evident peaks that give the ultraviolet (UL) and blue luminescence (BL) emission bands at (396) and (437) nm, respectively.

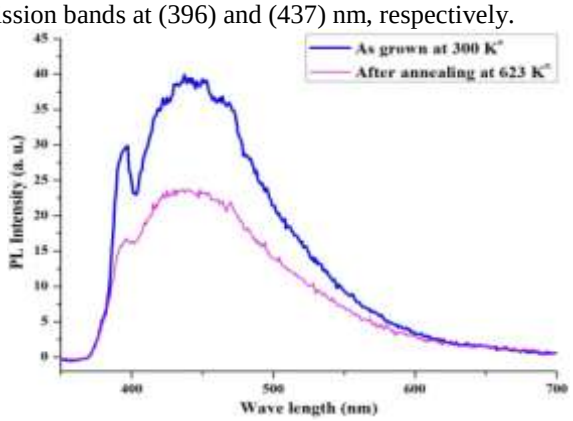


**Figure 11:** Room temperature Photoluminescence spectra of ZnS NPs films prepared and annealed at (300K) and (623K) respectively


Licensed Under Creative Commons Attribution CC BY

After annealing temperature at (623K), these bands were quenched and shifted to (397) and (439) nm, as shown in table 2.

**Table 2:** shows that, (UL) and (BL) of ZnS NPs films prepared at temperature (300k) and (623k)

| Preparing temp. (K) | PL | FWHM (nm) | Intensity | λ (nm) |
|---|---|---|---|---|
| As grown (300K) | UL | 62 | 29.8 | 396 |
| | BL | 111 | 38.6 | 437 |
| Annealing temp. (623K) | UL | 77.5 | 16.6 | 397 |
| | BL | 118 | 23.2 | 439 |

This emission bands originated from zinc oxide and sulfur vacancies. The quenching of (PL) was attributed to the oxidation of sulfur into sulfate and the removal of lattice defects by the annealing process.

## 4. Conclusion

1) From the absorbance spectra for ZnS thin films, we observed that the maximum absorption peaks shift towards the smaller wavelength with the increase of annealing temperatures. And the value of absorption and reflection decreases with the increases of annealing temperatures whereas the transmission increases.
2) The optical energy gap for ZnS increases with the increase of annealing temperatures.
3) Increasing number pulses of laser on the samples leads to increased roughness of the surface and increased temperature reduces.
4) ZnS NPs films at 300 $K^o$ and the transmittance increased after annealing at 623 K with increasing number pulses of laser.
5) With the increase of absorption, the grain size increases.
6) The surface was uniformly covered and the surface properties observed have a strong effect on the optical properties of thin films such as transition, absorption ,and reflection .
7) Absorption coefficient $(\alpha) > 10^4\ cm^{-1}$ indicates direct transitions.
8) Film annealing leads to improving crystallinity, increasing of the grain size and eliminating some defects from the films.
9) The carrier concentration decreases with the increase of annealing temperatures, and the carrier mobility increases with the increase of annealing temperatures.

## References

[1] A.Nitta , K. Tanakab, Y. Maekawab, M. Kusabirakib, and Masao Aozasa, Effects of gas impurities in the sputtering environment on the stoichiometry and crystallinity of ZnS:Mn electroluminescent-device active layers, Thin Solid Films. 384(2001), 261-268
[2] S.Yano, R.Schroeder, B.Ullrich, and H.Sakai, Absorption and photocurrent properties of thin ZnS films formed by pulsed-laser deposition on quartz, Thin Solid Films. 423(2003) 273–276
[3] Q.J. Feng, D.Z. Shen, J.Y. Zhang, H.W. Liang, D.X. Zhao, Y.M. Lua, and X.W. Fan, Highly aligned ZnS nanorods grown by plasma-assisted metalorganic chemical vapor deposition, J. Crystal Growth. 285(2005) 561–565
[4] S. Wang, X. Fu, G. Xia ,J. Wang, J. Shao, and Z. Fan, Structure and optical properties of ZnS thin films grown by glancing angle deposition, Appl. Surf. Sci., 252 (2006) 8734–8737
[5] N. Fathy, R. Kobayashi, and M. Ichimura, Preparation of ZnS thin films by the pulsed electrochemical deposition, Mater. Sci. Eng. B. 107(2004) 271–27
[6] P. Roy, J.R. Ota, and S.K. Srivastava, Crystalline ZnS thin films by chemical bath deposition method and its characterization, Thin Solid Films. 515(2006) 1912-1917
[7] Davidson WL, Xray diffraction evidence for ZnS formation in zinc activated rubber vulcanizates. phys Rev 74(1948) 116-117
[8] Biswas s, kar S, abrication of ZnS nanoparticles and nanorods with cubic and hexagonal crystal structures : a sample solvothermal approach, Nanotechnology. 19 (2008) 045710
[9] H wany D.Ahnj Huik, Huik, sony, Structural and optical Properties of ZnS thin films deposited by RF magnetron suputtering, Nanoscale Reslett. (2012) 7-26
[10] Hariskos D, Fuchs B, Menner R, Naghavi N, Hubertc, Lincot D, powalia M, The Zn(S,O,OH)/ZnMgo buffer in thin film Cu(In,Ga) (Se,S) 2-based solar cell part ll : magnetron suppttering of the ZnMgo buffer layer for in – line Co- evaporated Cu(In,Ga) Se2 solar cells prog photovolt pes" App 17 (2009) 479-488.
[11] Fxany xs,ye cH . peng xs , wang YH,WuYc, Zhang LD, Large- scale synthesis of ZnS nanosheets by the evaporation of ZnS nanopowders, J cryst Growth. 263 (2004) 263-268
[12] Wang xy, Zhu yc, Fan H, Zhang MF,XiBJ, wang HZ, Growth of ZnS Microfans and nanosheets : Controllable morphology and phase, J cryst Growth. 310 (2008) 2525-2531
[13] A. Ichiboshi, M. Hongo, T.Akamine, T.Dobashi, T. Nakada, Ultrasonic chemical bath depost of ZnS(O,OH) buffer layers and its application to CIGS thin film solar cells, sol energy mater So: cells. 90 (2006) 3130-3135
[14] A . Inamet, Low magnetic flux noise observed in laser deposited in situ films of yB2 Cu3Oy and implications for high – TC SQUIDS" . In: Nature 341 O,pp.(1980) 723 – 726
[15] W.H. Bloss, F. Plisterer, H.W. Schock, Advances in Solar energy, and Annual review of research & development. Vol. 4(1988) P-275
[16] C. Suryanarayana , M.G. Norton, X-ray diffraction a practical approach, New York: Plenum Press; 1998.
[17] M.Ethayaraja, C.Ravikumar, D. Muthukumaran, K.Dutta, R.J. Bandyopadhyaya , CdS-ZnS core-shell nanoparticle formation: Experiment mechanism and simulation, J. Phys. Chem. 111 (2007) 3246-3252


Licensed Under Creative Commons Attribution CC BY